




Surface-sensitive fragile twofold symmetry in the kagome-lattice superconductor CsV₃Sb₅

Chenxi Jiang ¹, Miaocong Li ¹, Yi Liu,^{1,2} Zheng Li,¹ Jinjin Wang,¹ Qian Tao,¹ Guang-Han Cao,^{1,3,4} and Zhu-An Xu ^{1,3,4,*}

¹Zhejiang Province Key Laboratory of Quantum Technology and Device, School of Physics, Zhejiang University, Hangzhou 310027, China

²Department of Applied Physics, Zhejiang University of Technology, Hangzhou 310023, China

³State Key Laboratory of Silicon and Advanced Semiconductor Materials, Zhejiang University, Hangzhou 310027, China

⁴Collaborative Innovation Centre of Advanced Microstructures, Nanjing University, Nanjing 210093, China



(Received 11 October 2022; revised 5 August 2023; accepted 7 August 2023; published 16 August 2023)

The newly discovered kagome superconductor CsV₃Sb₅ exhibits numerous exotic phenomena and offers a rare platform to study the interplay of topological state, charge-density wave order, and superconductivity. Here we systematically investigated the twofold symmetry in the superconducting state through the measurements of off-plane resistivity under in-plane rotating magnetic field. It is found that the distinct twofold symmetry exists in the superconducting phase. Furthermore, this symmetry breaking is very fragile and sensitive to the surface degradation. When the sample is exposed to the atmosphere for several days, the twofold symmetry tends to be weakened and eventually disappears with increasing exposing time. However, it can be recovered after sample surface exfoliation. Combined with other measurements, we propose that this fragile twofold symmetry should be related to the surface condition. The surface degradation may be caused by Cs atom vacancies on the surface, which could destroy the topological surface state. We discussed the possible relationship between the fragile twofold symmetry and the topological surface state discovered by recent angle-resolved photoemission spectroscopy experiments.

DOI: [10.1103/PhysRevB.108.054513](https://doi.org/10.1103/PhysRevB.108.054513)

I. INTRODUCTION

Kagome lattice, due to its unique structure, usually exhibits fascinating phenomena, such as flat bands as well as Dirac points [1,2]. For instance, the massive Dirac point was discovered in the kagome material Fe₃Sn₂ [3] and the quantum-limit Chern phase was realized in quantum magnet TbMn₆Sn₆ [4]. Recently, a family of new kagome lattice superconductors AV₃Sb₅ (A = K, Rb, Cs) has been discovered with $T_c \sim 0.9\text{--}3$ K and there coexists a kind of chiral charge density wave (CDW) order around 78–103 K [5–7]. The kagome lattice is composed of V atoms, and a 2×2 superlattice in CDW phase can be detected by the scanning tunneling microscopy (STM) measurements [8–14]. Furthermore, pronounced intensity anisotropy of charge modulation vector due to chiral charge order is revealed and the chirality can be modulated by the magnetic field [8]. Meanwhile, angle-resolved photoemission spectroscopy (ARPES) investigations indicate a highly anisotropic CDW gap and linear dispersion [15–20]. The resistivity measurement displays obvious quantum oscillation, and Berry phase $\sim \pi$ as well as small effective mass m^* can be extracted [7,16,21]. Although there has been no trace of long-ranged magnetic order or localized magnetic moments, giant anomalous Hall effect (AHE) is discovered in the low field region after subtracting the linear background, which may come from the contributions of large Berry curvature, extrinsic skew scattering, or chiral flux phase [22–25]. Moreover, the reported temperature-pressure phase diagram

of AV₃Sb₅ (A = K, Rb, Cs) shows two superconducting domes, which implies the complicated competition between superconductivity and CDW ordering [26–33]. Such a competition can also be tuned by chemical substitutions [34–36].

To date, several studies have uncovered the topological phase and topologically nontrivial surface states of AV₃Sb₅ (A = K, Rb, Cs) by density-functional theory (DFT) [37] and ARPES measurements [15,16,38]. CsV₃Sb₅ was first regarded as a Z₂ topological metal with superconducting ground state and then identified as the Dirac nodal line semimetal, which provides insights into the potential role of Dirac nodal loops in transport properties. In addition to DFT and ARPES results, there are other experimental signatures pointing to the unconventional superconducting state. The pair density wave (PDW) [10] and a robust zero-bias conductance peak resembling Majorana bound states on Cs surfaces have been observed by STM [39], consistent with the observation of charge-4e and charge-6e superconductivity in CsV₃Sb₅ nanodevices, which implies the unconventional superconductivity [40]. Despite two-gap s-wave symmetry and multiband nature in superconducting state are demonstrated by measuring the magnetic penetration depth, nuclear magnetic resonance (NMR), and muon spin rotation (μ SR) [41–47], the Josephson junction based on this material shows the spin-triplet supercurrent and spatially localized conducting channels [48]. These results call for further study to clarify the controversial superconducting state.

It has been theoretically proposed that odd-parity pairing symmetry exists in the topological superconductors (TSCs) [49]. The TSCs would exhibit unconventional properties, such as nematic superconductivity, which has been corroborated

*zhuan@zju.edu.cn

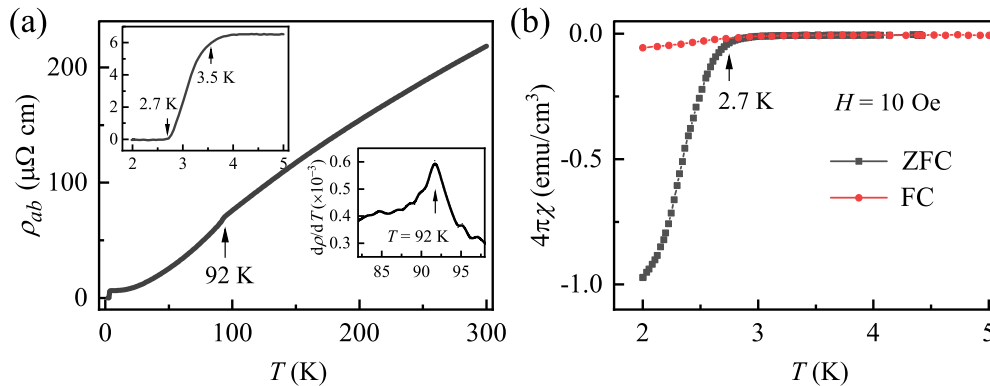


FIG. 1. (a) Temperature dependence of in-plane resistivity for the sample S1. Top left inset: expanded view of superconducting transition; right bottom inset: derivative of resistivity around CDW transition temperature. (b) Temperature dependence of magnetic susceptibility in the temperature range between 2 and 5 K. The black and red curve represents zero-field cooling (ZFC) and field cooling (FC), respectively.

in the candidates of TSCs, i.e., $\text{Cu}_x\text{Bi}_2\text{Se}_3$ and $\text{Sr}_x\text{Bi}_2\text{Se}_3$ [50,51]. They are obtained by doping topological insulator Bi_2Se_3 . The results of heat capacity, upper critical field [52], NMR [50] on $\text{Cu}_x\text{Bi}_2\text{Se}_3$ as well as angle-dependent resistivity on $\text{Sr}_x\text{Bi}_2\text{Se}_3$ [51,53] show distinct twofold symmetry, demonstrating odd-parity nematic phase. Latest transport measurements of the c -axis resistivity on CsV_3Sb_5 have discovered twofold symmetry of superconducting state [54,55], similar to the phenomenon observed in $\text{Sr}_x\text{Bi}_2\text{Se}_3$ [53]. However, the symmetry observed in CsV_3Sb_5 displays some differences. The twofold anisotropy exists even above the superconducting upper critical field and persists in the temperature range much higher than T_c , up to the CDW order temperature ~ 95 K. Therefore, it raises the question whether the twofold symmetry is caused by the intrinsic odd-parity superconductivity or influenced by the CDW ordering.

Here we carefully investigated the twofold symmetry by measuring the c -axis resistivity of CsV_3Sb_5 with magnetic field applied in the ab plane. In our experiments, we observed clear twofold symmetry in the superconducting state, which is consistent with previous reports [54]. Moreover, we found that the twofold symmetry of the resistivity is very fragile and sensitive to the surface degradation. After several days exposed to the atmosphere, the distinct twofold symmetry gradually degenerates and disappears in the end. However, the twofold symmetry is not observed in the angular dependence of magnetic susceptibility and no significant change in AHE is detected after the sample surface degradation. We propose that the fragile twofold symmetry should be a consequence of surface degradation which may be related to the Cs atom vacancies.

II. EXPERIMENTAL DETAILS

Single crystals of CsV_3Sb_5 are grown by the flux method [5]. The crystal structure is confirmed by the single-crystal x-ray diffraction (XRD) performed on the PANalytical x-ray diffractometer (Empyrean) with a $\text{Cu } K_{\alpha 1}$, and the chemical composition is detected by the energy dispersive x-ray spectroscopy (EDS). The magnetic susceptibility is measured on the Quantum Design Magnetic Properties Measurement System (MPMS - 5 T), using zero-field-cooling (ZFC) and

field-cooling (FC) protocol. The in-plane resistivity is measured using the standard four-terminal method. The resistivity of c axis is measured using the four-electrode method with the Corbino-shape-like configuration and the current is always applied along the c axis, as shown in the inset of Fig. 2(a). When performing rotation measurements, the magnetic field is applied in the ab plane.

Four samples labeled as S1, S2, S3, and S4 were measured in our experiments. The sample S1 was measured with fresh surface when it was cut from the as-grown single crystals, and then it was measured again as it was exposed to the atmosphere for about three months, to check the change of twofold symmetry in superconducting state. Interestingly, the twofold symmetry becomes unobservable after exposing to the atmosphere. After exfoliating the sample S1 to obtain the fresh surfaces, the twofold symmetry recovers. A more careful investigation on the evolution of the twofold symmetry with time was performed on the sample S2 on which we measured the twofold symmetry several times during the period of about two months exposed to the atmosphere. The sample S3 (from the same batch as S1 and S2) was selected to measure Hall effect and the evolution of anomalous Hall effect vs. surface degradation. The sample S4 with fresh surface from the same batch as S2 was selected to measure the angular dependence of magnetization. All the transport measurements are performed on the Physical Properties Measurement System (PPMS-DynaCool) equipped with the rotation probe option.

III. RESULTS AND DISCUSSIONS

To achieve a more distinct hierarchy, this section is organized as the following: Sec. III A presents the basic superconducting properties and the twofold symmetry observed in the sample S1 with fresh surface; in Sec. III B, a sequence of experiments on the sample S2 are presented to study the evolution of twofold symmetry with surface degradation; Sec. III C contains the measurements on the angular-dependent magnetization of the sample S4 and AHE of the sample S3 (both from the same batch of sample S2) to show that the fragile twofold symmetry is mainly related to the surface property; and then in Sec. III D we discussed the

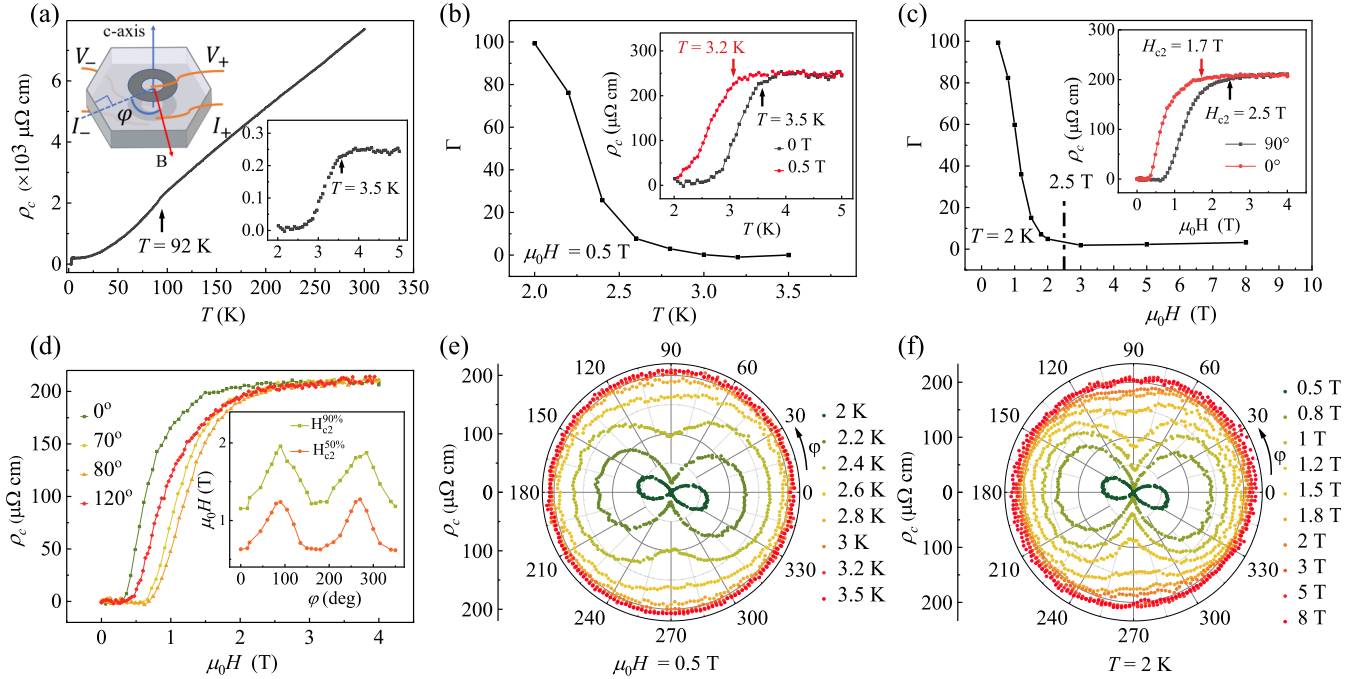


FIG. 2. (a) Temperature dependence of c -axis resistivity for the sample S1. Inset: schematic diagram of the c -axis resistivity measurement. $\varphi = 0^\circ$ corresponds to H perpendicular to the sample hexagonal side. (b) Temperature dependence of Γ . Inset: expanded view of superconducting transition under zero field and 0.5 T. (c) Field dependence of Γ . Inset: expanded view of superconducting transition at 0° and 90° . (d) Magnetic field dependence of c -axis resistivity at four representative angles at $T = 2$ K. Inset: extracted upper critical field at different angles using two criterions, i.e., 90% and 50% of the resistivity transitions under $\mu_0 H = 4$ T. (e) Angular dependence of c -axis resistivity of different temperatures under fixed magnetic field $\mu_0 H = 0.5$ T. (f) Angular dependence of c -axis resistivity under different magnetic fields at fixed temperature $T = 2$ K.

possible explanation of the fragile twofold symmetry and its possible connection with topological surface state.

A. Basic superconducting properties and twofold symmetry

Figures 1(a) and 1(b) display the basic superconducting properties of the sample S1. From the in-plane resistivity shown in Fig. 1(a), we can observe a kink related to the CDW transition around 92 K as well as a superconducting transition at T_c of about 2.7 K (defined as the zero-resistivity temperature), which is better observed from the enlarged view in the inset of Fig. 1(a). These properties are consistent with the literatures [15,23]. The temperature dependence of magnetic susceptibility is presented in Fig. 1(b). Clear diamagnetism signals below about 2.7 K are observed in the measurements of both ZFC and FC under the magnetic field $H = 10$ Oe, consistent with the resistivity measurements. The estimated superconducting shielding volume fraction based on the ZFC curve is nearly 100%, implying good quality of the sample.

Figure 2 displays the main result of twofold symmetry for the sample S1 with fresh surface. Figure 2(a) shows the temperature dependence of c -axis resistivity. Both a superconducting transition and a weak CDW transition are observed at 2.7 K and 92 K, respectively, consistent with the result of in-plane resistivity. The inset in Fig. 2(a) shows a schematic diagram of c -axis resistivity measurements. In order to probe the possible twofold symmetry in superconducting properties, we measured the resistivity along the c axis while the magnetic field was rotating in the ab plane to avoid possible

anisotropy caused by the Lorentz force between the current and the magnetic field. Considering the crystal structure of CsV_3Sb_5 , i.e., $P6/mmm$ space group, the c -axis resistivity is expected to show either sixfold symmetry or no discernable periodicity if the anisotropy due to the nematic superconductivity is absent. As shown in Figs. 2(e) and 2(f), a clear twofold symmetry in the c -axis resistivity is observed, reminiscent of the result of doped topological insulator $\text{Sr}_{0.10}\text{Bi}_2\text{Se}_3$, which has been proposed to be a potential TSC [51]. Under magnetic field $\mu_0 H = 0.5$ T [see Fig. 2(e)], a distinct drumhead shape curve emerges at low temperatures, demonstrating the twofold symmetry directly. The distinct drumhead shape degenerates gradually with increasing temperature. It becomes an ellipse around 2.6 K and eventually becomes a circle above $T_c \sim 3.2$ K. To quantitatively describe the twofold symmetry, we define a parameter $\Gamma = (\rho_{0^\circ} + \rho_{180^\circ} - \rho_{90^\circ} - \rho_{270^\circ}) / (\rho_{0^\circ} + \rho_{90^\circ} + \rho_{180^\circ} + \rho_{270^\circ}) \times 100\%$. The temperature dependence of Γ tends downward as temperature increases and Γ becomes nearly zero above 3 K, as shown in Fig. 2(b). This indicates the absence of twofold symmetry above T_c , compared with the temperature dependence of resistivity under $\mu_0 H = 0.5$ T (red points) shown in the inset of Fig. 2(b). The behavior is similar in the case of fixed temperature when varying the magnetic field. At a fixed temperature T of 2 K, the distinct drumhead shape curve is revealed with small magnetic field, then it gradually weakens with increasing magnetic field and finally becomes a circular shape, as shown in Fig. 2(f). The value of Γ decreases sharply below 2 T and the twofold symmetry is not very obvious beyond its upper critical field

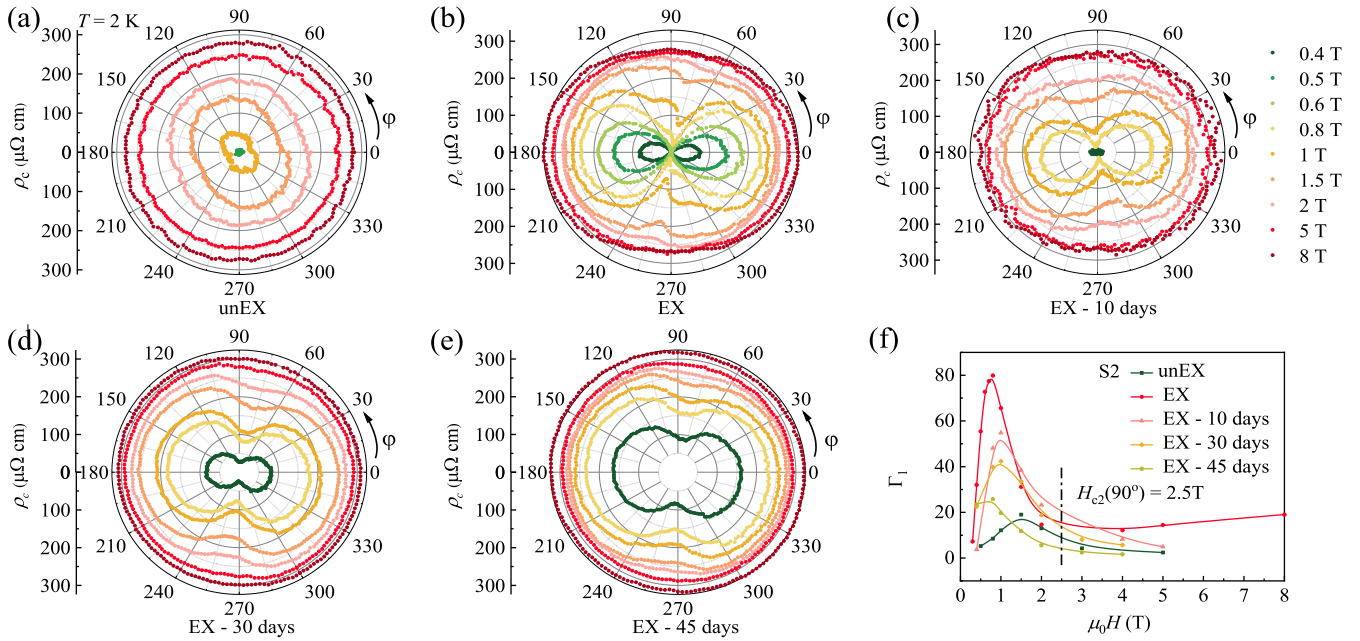


FIG. 3. Twofold symmetry of the sample S2 at $T = 2$ K under different surface conditions. (a) Unexfoliated surface (exposed in atmosphere for a few months and measured without exfoliation), (b) fresh exfoliated surface, and then placed in the atmosphere for (c) 10 days, (d) 30 days, (e) 45 days. (f) Field dependence of Γ_1 at $T = 2$ K under different surface conditions. Here “EX” stands for exfoliation.

(H_{c2}) as shown in Fig. 2(c). It should be noted that experiments conducted on $\text{Nb}_x\text{Bi}_2\text{Se}_3$ and $\text{Cu}_x\text{Bi}_2\text{Se}_3$ discovered the signature of nematic phase fluctuations [56], in accord with the theoretic work [57]. However, the distinct twofold symmetry does not exist above but near T_c in this study, displaying no observable signature of nematic phase fluctuations. In contrast with the antiphase twofold symmetric feature far above H_{c2} reported in the previous study [54], the absence of distinct symmetry under high field should most likely be due to the strong disorders in our samples, which can be revealed by the quite small magnetoresistance in the normal state.

In order to further confirm the twofold symmetry, we also measured the magnetic field dependence of resistivity at some selected field directions at $T = 2$ K. Figure 2(d) exhibits the results of some representative field angles. All the curves merge together in the low and high magnetic field region, except the intermediate region. In the intermediate region, the resistivity at zero degree angle ($\varphi = 0$) is the first one to increase around H of 0.4 T, indicating the lowest H_{c2} , while the resistivity of 80 degree starts to increase about H of 0.7 T. The large disparity between different angles clearly indicates twofold symmetry. To have a more intuitive view, the extracted upper critical field is shown in the inset of Fig. 2(d), which adopts two criterions. The upper critical field defined as 90% and 50% of resistivity under 4 T show evident twofold symmetry, indicating the superconducting gap also exhibits twofold symmetry, which indicates the possible nematic superconductivity. Both of the upper critical field show peaks near 90° and 270° .

B. Evolution of twofold symmetry

In addition to the general twofold symmetry properties described above, we found that this twofold symmetry below

T_c is fragile to the sample surface condition, demonstrated by the fact that the twofold symmetry of the sample S1 disappears after about three months stocking in a dry box while T_c of this sample does not change. It is very interesting that the twofold symmetry of the sample S1 recovers after surface exfoliation. In order to further elucidate this phenomenon, we selected the sample S2, which has been exposed to atmosphere for four months to perform a series of experiments. Figure 3(a) shows the initial pattern of angle dependence of ρ_c for the sample S2. Under low magnetic field, it shows elliptical shape, in contrast to the drumhead shape as shown in Fig. 2(e). This shape is similar to the result found in $\text{Ba}_{0.65}\text{K}_{0.35}\text{Fe}_2\text{As}_2$ where an s -wave pairing symmetry is proposed and thus the in-plane H_{c2} should be isotropic [53], indicating the twofold symmetry is absent. The tiny differences between two directions may be due to the slight misalignment of electrodes in the top and bottom surfaces. Then we exfoliated the sample S2 to obtain the fresh surface, as a result, the twofold symmetry recovers as shown in Fig. 3(b), indicating a possible connection between the twofold symmetry and the surface condition. Then we measured the exfoliated S2 after a period of time to study the evolution of twofold symmetry with sample surface degradation. Figures 3(c)–3(e) shows the results after 10 days, 30 days, and 45 days, respectively. After several days placed in the atmosphere, the twofold symmetry becomes weak. In order to avoid enlarged uncertainty in the defined anisotropic parameter Γ due to the small residual resistance as temperature close to T_c , we revised the definition of the anisotropic parameter as $\Gamma_1 = (R_{\max} - R_{\min})/R_{T=4\text{K}} \times 100\%$. For a better view of the evolution of the twofold symmetry with time, we plot Γ_1 vs. magnetic field in Fig. 3(f). Obviously Γ_1 decreases gradually with stocking time after the sample exfoliation. This fascinating phenomenon implies that the possible nematic

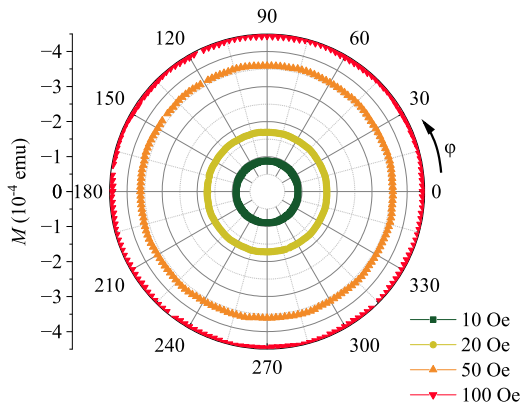


FIG. 4. Angular dependence of magnetization under in-plane rotating magnetic field at fixed temperature $T = 2$ K for sample S4.

superconductivity reflected by the twofold symmetry is fragile and may be intimately related to the surface condition.

C. Magnetic susceptibility and anomalous Hall effect

There is another possibility that the twofold symmetry is mainly related to the bulk property. In such a scenario, the deteriorated superconducting surface may lead to the weakening of superconductivity along the c axis, and thus it could result in a weaker twofold symmetry. To check this possibility, we further measured the angular dependence of magnetization at $T = 2$ K with magnetic field rotating in the plane on the sample S4 (from the same batch as S2) as shown in Fig. 4. The magnetization is generally more indicative of the properties of the bulk state. We did not observe any significant twofold symmetry in magnetization, which exhibits nearly angular independent. This result is rather different from the spontaneous rotational symmetry breaking in the superconducting magnetic response of Nb-doped Bi_2Se_3 [58]. All these data imply that the twofold symmetry may mainly be related to the surface property while we cannot rule out the influence of bulk property completely.

Moreover, since there is a close relationship between CDW and superconductivity, it is reasonable that the twofold symmetry and its evolution may be derived from CDW ordering. Therefore, we also performed careful measurements to check possible change in superconductivity and CDW state of the sample S2. By measuring the in-plane resistivity, we cannot observe any obvious changes in the CDW ordering temperature and superconducting transition temperature of the sample S2 with different exposing time, as shown in Fig. 5(a). This suggests that the possible nematic superconducting phase should be affected by the sample surface condition directly rather than the CDW ordering. In addition, we employed a series of AHE measurements on the sample S3, which is from the same batch of the sample S2 to investigate the possible evolution of AHE with time, as shown in Fig. 5(b). The quite large AHE in this material is proposed to be a consequence of the so-called chiral CDW ordering and thus it is a characteristic feature of the chiral CDW state [23]. There is no obvious change in the AHE curves with increasing exposing time, which implies that the twofold symmetry and CDW order have different origins. Yet the fact that both AHE and

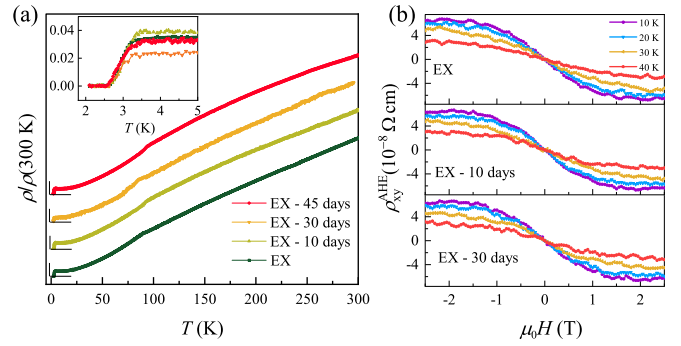


FIG. 5. (a) Temperature-dependent normalized resistivity of exfoliated sample S2 with different exposure time. The offset is applied for a better recognition among the different curves. Inset: expanded view of superconducting transition. (b) Field-dependent AHE of exfoliated sample S3.

CDW remain unchanged implies there is a positive correlation between them.

Overall, our data show that there is no apparent twofold symmetry in the magnetization, which is regarded as a bulk superconducting property. AHE does not change obviously over time either, which implies that the sample aging mainly affects the surface property and has little influence on the bulk property. In other words, the results of AHE and the magnetization further imply that the twofold symmetry should be primarily related to the surface property.

D. Discussions

Considering the strong dependence of the twofold symmetry on the sample surface condition, we thus discuss the possible connection between topological surface state and the twofold symmetry. Recent ARPES experiment has discovered the signature of quantum confinement related to surface state [16]. Combined with the DFT calculations, they found this novel phenomenon mainly comes from the topmost two layers of the surface and surface Dirac cone induced by the quantum-well state. A previous report on PbTaSe_2 has observed the existence of twofold symmetry in the resistive upper critical field and point-contact spectra measurements but it is absent in the specific heat measurement, indicating surface-only electronic nematicity [59]. Combined with the study on PbTaSe_2 , we can reasonably argue that the nematic superconductivity may exist in surface states in CsV_3Sb_5 as well as in PbTaSe_2 . However, further experiment is required to verify this point.

To further verify that the fragile twofold symmetry is sensitive to the surface degradation, there are other corroborated experimental studies. Recent ARPES study conducted by Huai *et al.* has discovered the band evolution with time [19]. They proposed that the α band varies with time due to the increasing Cs vacancies on the surface. This kind of Cs vacancy is also elucidated in the investigation of selective oxidized CsV_3Sb_5 thin flakes [60]. In addition, ARPES experiments have also revealed the surface state attributed to the Cs terminated surface [61]. Therefore, these findings support the possible existence of the Cs vacancies, which may cause the surface degradation and account for the evolution

of twofold symmetry with sample aging. It may also naturally explain that the twofold symmetry is only observed in the resistivity measurement, unlike $\text{Cu}_x\text{Bi}_2\text{Se}_3$ where various bulk-sensitive probes such as heat capacity and NMR have observed the twofold symmetry [50,52]. Such a surface-sensitive symmetry breaking has also been reported in other materials. For instance, a previous AC susceptibility experiment on the topologically nontrivial superconductor In_2Sb has found a Meissner-like signal above H_{c2} , which is demonstrated to be consistent with the surface superconductivity modified by topological surface states. Moreover, the anomalous behavior mentioned above has a deep relationship with its surface in this material [62]. Once the surface structure is damaged and/or not complete, the Meissner-like signal above H_{c2} becomes weaker or even disappears. This implies the sensitivity of surface superconductivity to the surface condition, which also coincides with our results. In another example, surface superconductivity in the TaIrTe_4 could be influenced by surface degradation, which is reflected by the discrepancy in critical current [63].

IV. CONCLUSION

In conclusion, we carefully designed experiments on the twofold symmetry in the superconducting state of CsV_3Sb_5 by measuring the c -axis resistivity with rotating in-plane magnetic field. It is discovered that the distinct twofold

symmetry exists below T_c , and the symmetry smears out with the increase of temperature and finally disappears above T_c . Moreover, the twofold symmetry is intimately related to the surface condition. It weakens and eventually vanishes with increasing exposure duration when the sample is exposed to the atmosphere. Nevertheless, it can be recovered by following exfoliation. Combined with the measurements of magnetization as well as AHE, the fragile twofold symmetry should be associated with the surface property. The evolution and disappearance of this fragile twofold symmetry could be attributed to the surface degradation, which is likely caused by the Cs atom vacancies on the surface. However, whether the twofold symmetry is a feature of the surface superconductivity or even the topological surface state needs further study to clarify. This fascinating phenomenon, combined with its other novel properties, implies this material is a rare platform to explore the unconventional superconductivity.

ACKNOWLEDGMENTS

This work was supported by the National Key R&D Program of the China (Grant No. 2019YFA0308602), the National Science Foundation of China (Grant No. 12174334), the Key R&D Program of Zhejiang Province in China (Grant No. 2021C01002), and the Fundamental Research Funds for the Central Universities of China.

-
- [1] G. Xu, B. Lian, and S.-C. Zhang, Intrinsic Quantum Anomalous Hall Effect in the Kagome Lattice $\text{Cs}_2\text{LiMn}_3\text{F}_{12}$, *Phys. Rev. Lett.* **115**, 186802 (2015).
- [2] K. Ohgushi, S. Murakami, and N. Nagaosa, Spin anisotropy and quantum Hall effect in the kagomé lattice: Chiral spin state based on a ferromagnet, *Phys. Rev. B* **62**, R6065 (2000).
- [3] L. Ye, M. Kang, J. Liu, F. von Cube, C. R. Wicker, T. Suzuki, C. Jozwiak, A. Bostwick, E. Rotenberg, D. C. Bell, L. Fu, R. Comin, and J. G. Checkelsky, Massive Dirac fermions in a ferromagnetic kagome metal, *Nature (London)* **555**, 638 (2018).
- [4] J.-X. Yin, W. Ma, T. A. Cochran, X. Xu, S. S. Zhang, H.-J. Tien, N. Shumiya, G. Cheng, K. Jiang, B. Lian, Z. Song, G. Chang, I. Belopolski, D. Multer, M. Litskevich, Z.-J. Cheng, X. P. Yang, B. Swidler, H. Zhou, H. Lin *et al.*, Quantum-limit Chern topological magnetism in TbMn_6Sn_6 , *Nature (London)* **583**, 533 (2020).
- [5] B. R. Ortiz, L. C. Gomes, J. R. Morey, M. Winiarski, M. Bordelon, J. S. Mangum, I. W. H. Oswald, J. A. Rodriguez-Rivera, J. R. Neilson, S. D. Wilson, E. Ertekin, T. M. McQueen, and E. S. Toberer, New kagome prototype materials: discovery of KV_3Sb_5 , RbV_3Sb_5 , and CsV_3Sb_5 , *Phys. Rev. Mater.* **3**, 094407 (2019).
- [6] B. R. Ortiz, P. M. Sarte, E. M. Kenney, M. J. Graf, S. M. L. Teicher, R. Seshadri, and S. D. Wilson, Superconductivity in the Z_2 kagome metal KV_3Sb_5 , *Phys. Rev. Mater.* **5**, 034801 (2021).
- [7] Q. Yin, Z. Tu, C. Gong, Y. Fu, S. Yan, and H. Lei, Superconductivity and normal state properties of kagome metal RbV_3Sb_5 single crystals, *Chin. Phys. Lett.* **38**, 037403 (2021).
- [8] Y.-X. Jiang, J.-X. Yin, M. M. Denner, N. Shumiya, B. R. Ortiz, G. Xu, Z. Guguchia, J. He, M. S. Hossain, X. Liu, J. Ruff, L. Kautzsch, S. S. Zhang, G. Chang, I. Belopolski, Q. Zhang, T. A. Cochran, D. Multer, M. Litskevich, Z.-J. Cheng *et al.*, Unconventional chiral charge order in kagome superconductor KV_3Sb_5 , *Nat. Mater.* **20**, 1353 (2021).
- [9] N. Shumiya, M. S. Hossain, J.-X. Yin, Y.-X. Jiang, B. R. Ortiz, H. Liu, Y. Shi, Q. Yin, H. Lei, S. S. Zhang, G. Chang, Q. Zhang, T. A. Cochran, D. Multer, M. Litskevich, Z.-J. Cheng, X. P. Yang, Z. Guguchia, S. D. Wilson, and M. Z. Hasan, Intrinsic nature of chiral charge order in the kagome superconductor RbV_3Sb_5 , *Phys. Rev. B* **104**, 035131 (2021).
- [10] H. Chen, H. Yang, B. Hu, Z. Zhao, J. Yuan, Y. Xing, G. Qian, Z. Huang, G. Li, Y. Ye, S. Ma, S. Ni, H. Zhang, Q. Yin, C. Gong, Z. Tu, H. Lei, H. Tan, S. Zhou, C. Shen *et al.*, and Roton pair density wave in a strong-coupling kagome superconductor, *Nature (London)* **599**, 222 (2021).
- [11] H.-S. Xu, Y.-J. Yan, R. Yin, W. Xia, S. Fang, Z. Chen, Y. Li, W. Yang, Y. Guo, and D.-L. Feng, Multiband Superconductivity with Sign-Preserving Order Parameter in Kagome Superconductor CsV_3Sb_5 , *Phys. Rev. Lett.* **127**, 187004 (2021).
- [12] H. Li, H. Zhao, B. R. Ortiz, T. Park, M. Ye, L. Balents, Z. Wang, S. D. Wilson, and I. Zeljkovic, Rotation symmetry breaking in the normal state of a kagome superconductor KV_3Sb_5 , *Nat. Phys.* **18**, 265 (2022).
- [13] H. Zhao, H. Li, B. R. Ortiz, S. M. Teicher, T. Park, M. Ye, Z. Wang, L. Balents, S. D. Wilson, and I. Zeljkovic, Cascade of correlated electron states in the kagome superconductor CsV_3Sb_5 , *Nature (London)* **599**, 216 (2021).
- [14] Z. Wang, Y.-X. Jiang, J.-X. Yin, Y. Li, G.-Y. Wang, H.-L. Huang, S. Shao, J. Liu, P. Zhu, N. Shumiya, M. S. Hossain, H. Liu, Y. Shi, J. Duan, X. Li, G. Chang, P. Dai, Z. Ye, G. Xu,

- Y. Wang *et al.*, Electronic nature of chiral charge order in the kagome superconductor CsV₃Sb₅, *Phys. Rev. B* **104**, 075148 (2021).
- [15] B. R. Ortiz, S. M. L. Teicher, Y. Hu, J. L. Zuo, P. M. Sarte, E. C. Schueller, A. M. Milinda Abeykoon, M. J. Krogstad, S. Rosenkranz, R. Osborn, R. Seshadri, L. Balents, J. He, and S. D. Wilson, CsV₃Sb₅: A Z₂ Topological Kagome Metal with a Superconducting Ground State, *Phys. Rev. Lett.* **125**, 247002 (2020).
- [16] Y. Cai, Y. Wang, Z. Hao, Y. Liu, X.-M. Ma, Z. Shen, Z. Jiang, Y. Yang, W. Liu, Q. Jiang, Z. Liu, M. Ye, D. Shen, Z. Sun, J. Chen, L. Wang, C. Liu, J. Lin, J. Wang, B. Huang *et al.*, Emergence of quantum confinement in topological Kagome superconductor CsV₃Sb₅ family, [arXiv:2109.12778](https://arxiv.org/abs/2109.12778).
- [17] Z. Wang, S. Ma, Y. Zhang, H. Yang, Z. Zhao, Y. Ou, Y. Zhu, S. Ni, Z. Lu, H. Chen, K. Jiang, L. Yu, Y. Zhang, X. Dong, J. Hu, H.-J. Gao, and Z. Zhao, Distinctive momentum dependent charge-density-wave gap observed in CsV₃Sb₅ superconductor with topological Kagome lattice, [arXiv:2104.05556](https://arxiv.org/abs/2104.05556).
- [18] K. Nakayama, Y. Li, T. Kato, M. Liu, Z. Wang, T. Takahashi, Y. Yao, and T. Sato, Multiple energy scales and anisotropic energy gap in the charge-density-wave phase of the kagome superconductor CsV₃Sb₅, *Phys. Rev. B* **104**, L161112 (2021).
- [19] L. Huai, Y. Luo, S. M. L. Teicher, B. R. Ortiz, K. Wang, S. Peng, Z. Wei, J. Shen, B. Wang, Y. Miao, X. Sun, Z. Ou, S. D. Wilson, and J. He, Surface-induced orbital-selective band reconstruction in kagome superconductor CsV₃Sb₅, *Chin. Phys. B* **31**, 057403 (2022).
- [20] Z. Liu, N. Zhao, Q. Yin, C. Gong, Z. Tu, M. Li, W. Song, Z. Liu, D. Shen, Y. Huang, K. Liu, H. Lei, and S. Wang, Charge-Density-Wave-Induced Bands Renormalization and Energy Gaps in a Kagome Superconductor RbV₃Sb₅, *Phys. Rev. X* **11**, 041010 (2021).
- [21] Y. Fu, N. Zhao, Z. Chen, Q. Yin, Z. Tu, C. Gong, C. Xi, X. Zhu, Y. Sun, K. Liu, and H. Lei, Quantum Transport Evidence of Topological Band Structures of Kagome Superconductor CsV₃Sb₅, *Phys. Rev. Lett.* **127**, 207002 (2021).
- [22] S.-Y. Yang, Y. Wang, B. R. Ortiz, D. Liu, J. Gayles, E. Derunova, R. Gonzalez-Hernandez, L. Šmejkal, Y. Chen, S. S. P. Parkin, S. D. Wilson, E. S. Toberer, T. McQueen, and M. N. Ali, Giant, unconventional anomalous Hall effect in the metallic frustrated magnet candidate, KV₃Sb₅, *Sci. Adv.* **6**, eabb6003 (2020).
- [23] F. H. Yu, T. Wu, Z. Y. Wang, B. Lei, W. Z. Zhuo, J. J. Ying, and X. H. Chen, Concurrence of anomalous Hall effect and charge density wave in a superconducting topological kagome metal, *Phys. Rev. B* **104**, L041103 (2021).
- [24] G. Zheng, C. Tan, Z. Chen, M. Wang, X. Zhu, S. Albarakati, M. Algarni, J. Partridge, L. Farrar, J. Zhou, W. Ning, M. Tian, M. S. Fuhrer, and L. Wang, Electrically controlled superconductor-to-failed insulator transition and giant anomalous Hall effect in kagome metal CsV₃Sb₅ nanoflakes, *Nat. Commun.* **14**, 678 (2023).
- [25] X. Feng, K. Jiang, Z. Wang, and J. Hu, Chiral flux phase in the Kagome superconductor AV₃Sb₅, *Sci. Bull.* **66**, 1384 (2021).
- [26] K. Y. Chen, N. N. Wang, Q. W. Yin, Y. H. Gu, K. Jiang, Z. J. Tu, C. S. Gong, Y. Uwatoko, J. P. Sun, H. C. Lei, J. P. Hu, and J. G. Cheng, Double Superconducting Dome and Triple Enhancement of T_c in the Kagome Superconductor CsV₃Sb₅ under High Pressure, *Phys. Rev. Lett.* **126**, 247001 (2021).
- [27] F. Du, S. Luo, B. R. Ortiz, Y. Chen, W. Duan, D. Zhang, X. Lu, S. D. Wilson, Y. Song, and H. Yuan, Pressure-induced double superconducting domes and charge instability in the kagome metal KV₃Sb₅, *Phys. Rev. B* **103**, L220504 (2021).
- [28] C. C. Zhao, L. S. Wang, W. Xia, Q. W. Yin, J. M. Ni, Y. Y. Huang, C. P. Tu, Z. C. Tao, Z. J. Tu, C. S. Gong, H. C. Lei, Y. F. Guo, X. F. Yang, and S. Y. Li, Nodal superconductivity and superconducting domes in the topological Kagome metal CsV₃Sb₅, [arXiv:2102.08356](https://arxiv.org/abs/2102.08356).
- [29] C. C. Zhu, X. F. Yang, W. Xia, Q. W. Yin, L. S. Wang, C. C. Zhao, D. Z. Dai, C. P. Tu, B. Q. Song, Z. C. Tao, Z. J. Tu, C. S. Gong, H. C. Lei, Y. F. Guo, and S. Y. Li, Double-dome superconductivity under pressure in the V-based kagome metals AV₃Sb₅ (A = Rb and K), *Phys. Rev. B* **105**, 094507 (2022).
- [30] F. H. Yu, D. H. Ma, W. Z. Zhuo, S. Q. Liu, X. K. Wen, B. Lei, J. J. Ying, and X. H. Chen, Unusual competition of superconductivity and charge-density-wave state in a compressed topological kagome metal, *Nat. Commun.* **12**, 3645 (2021).
- [31] X. Chen, X. Zhan, X. Wang, J. Deng, X.-B. Liu, X. Chen, J.-G. Guo, and X. Chen, Highly robust reentrant superconductivity in CsV₃Sb₅ under pressure, *Chin. Phys. Lett.* **38**, 057402 (2021).
- [32] Z. Zhang, Z. Chen, Y. Zhou, Y. Yuan, S. Wang, J. Wang, H. Yang, C. An, L. Zhang, X. Zhu, Y. Zhou, X. Chen, J. Zhou, and Z. Yang, Pressure-induced reemergence of superconductivity in the topological kagome metal CsV₃Sb₅, *Phys. Rev. B* **103**, 224513 (2021).
- [33] Q. Wang, P. Kong, W. Shi, C. Pei, C. Wen, L. Gao, Y. Zhao, Q. Yin, Y. Wu, G. Li, H. Lei, J. Li, Y. Chen, S. Yan, and Y. Qi, Charge density wave orders and enhanced superconductivity under pressure in the kagome metal CsV₃Sb₅, *Adv. Mater.* **33**, 2102813 (2021).
- [34] Y. M. Oey, B. R. Ortiz, F. Kaboudvand, J. Frassinetti, E. Garcia, R. Cong, S. Sanna, V. F. Mitrović, R. Seshadri, and S. D. Wilson, Fermi level tuning and double-dome superconductivity in the kagome metal CsV₃Sb_{5-x}Sn_x, *Phys. Rev. Mater.* **6**, L041801 (2022).
- [35] Y. Liu, Y. Wang, Y. Cai, Z. Hao, X.-M. Ma, L. Wang, C. Liu, J. Chen, L. Zhou, J. Wang, S. Wang, H. He, Y. Liu, S. Cui, J. Wang, B. Huang, C. Chen, and J.-W. Mei, Doping evolution of superconductivity, charge order and band topology in hole-doped topological kagome superconductors Cs(V_{1-x}Ti_x)₃Sb₅, *Phys. Rev. Mater.* **7**, 064801 (2023).
- [36] H. Yang, Y. Zhang, Z. Huang, Z. Zhao, J. Shi, G. Qian, B. Hu, Z. Lu, H. Zhang, C. Shen, X. Lin, Z. Wang, S. J. Pennycook, H. Chen, X. Dong, W. Zhou, and H.-J. Gao, Titanium doped kagome superconductor CsV_{3-x}Ti_xSb₅ and two distinct phases, *Sci. Bull.* **67**, 2176 (2022).
- [37] H. Tan, Y. Liu, Z. Wang, and B. Yan, Charge Density Waves and Electronic Properties of Superconducting Kagome Metals, *Phys. Rev. Lett.* **127**, 046401 (2021).
- [38] Z. Hao, Y. Cai, Y. Liu, Y. Wang, X. Sui, X.-M. Ma, Z. Shen, Z. Jiang, Y. Yang, W. Liu, Q. Jiang, Z. Liu, M. Ye, D. Shen, Y. Liu, S. Cui, J. Chen, L. Wang, C. Liu, J. Lin *et al.*, Dirac nodal lines and nodal loops in the topological kagome superconductor CsV₃Sb₅, *Phys. Rev. B* **106**, L081101 (2022).
- [39] Z. Liang, X. Hou, F. Zhang, W. Ma, P. Wu, Z. Zhang, F. Yu, J.-J. Ying, K. Jiang, L. Shan, Z. Wang, and X. H. Chen, Three-Dimensional Charge Density Wave and Surface-Dependent

- Vortex-Core States in a Kagome Superconductor CsV_3Sb_5 , *Phys. Rev. X* **11**, 031026 (2021).
- [40] J. Ge, P. Wang, Y. Xing, Q. Yin, H. Lei, Z. Wang, and J. Wang, Discovery of charge-4e and charge-6e superconductivity in kagome superconductor CsV_3Sb_5 , [arXiv:2201.10352](https://arxiv.org/abs/2201.10352).
- [41] W. Duan, Z. Nie, S. Luo, F. Yu, B. R. Ortiz, L. Yin, H. Su, F. Du, A. Wang, Y. Chen, X. Lu, J. Ying, S. D. Wilson, X. Chen, Y. Song, and H. Yuan, Nodeless superconductivity in the kagome metal CsV_3Sb_5 , *Sci. China Phys. Mech. Astron.* **64**, 107462 (2021).
- [42] C. Mu, Q. Yin, Z. Tu, C. Gong, H. Lei, Z. Li, and J. Luo, S-Wave superconductivity in kagome metal CsV_3Sb_5 revealed by $^{121/123}\text{Sb}$ NQR and ^{51}V NMR measurements, *Chin. Phys. Lett.* **38**, 077402 (2021).
- [43] D. Song, L. Zheng, F. Yu, J. Li, L. Nie, M. Shan, D. Zhao, S. Li, B. Kang, Z. Wu, Y. Zhou, K. Sun, K. Liu, X. Luo, Z. Wang, J. Ying, X. Wan, T. Wu, and X. Chen, Orbital ordering and fluctuations in a kagome superconductor CsV_3Sb_5 , *Sci. China Phys. Mech. Astron.* **65**, 247462 (2022).
- [44] E. M. Kenney, B. R. Ortiz, C. Wang, S. D. Wilson, and M. J. Graf, Absence of local moments in the kagome metal KV_3Sb_5 as determined by muon spin spectroscopy, *J. Phys.: Condens. Matter* **33**, 235801 (2021).
- [45] L. Yu, C. Wang, Y. Zhang, M. Sander, S. Ni, Z. Lu, S. Ma, Z. Wang, Z. Zhao, H. Chen, K. Jiang, Y. Zhang, H. Yang, F. Zhou, X. Dong, S. L. Johnson, M. J. Graf, J. Hu, H.-J. Gao, and Z. Zhao, Evidence of a hidden flux phase in the topological kagome metal CsV_3Sb_5 , [arXiv:2107.10714](https://arxiv.org/abs/2107.10714).
- [46] R. Gupta, D. Das, C. H. Mielke III, Z. Guguchia, T. Shiroka, C. Baines, M. Bartkowiak, H. Luetkens, R. Khasanov, Q. Yin, Z. Tu, C. Gong, and H. Lei, Microscopic evidence for anisotropic multigap superconductivity in the CsV_3Sb_5 kagome superconductor, *npj Quantum Mater.* **7**, 49 (2022).
- [47] C. Mielke III, D. Das, J.-X. Yin, H. Liu, R. Gupta, Y.-X. Jiang, M. Medarde, X. Wu, H. Lei, J. Chang, P. Dai, Q. Si, H. Miao, R. Thomale, T. Neupert, Y. Shi, R. Khasanov, M. Z. Hasan, H. Luetkens, and Z. Guguchia, Time-reversal symmetry-breaking charge order in a kagome superconductor, *Nature (London)* **602**, 245 (2022).
- [48] Y. Wang, S. Yang, P. K. Sivakumar, B. R. Ortiz, S. M. L. Teicher, H. Wu, A. K. Srivastava, C. Garg, D. Liu, S. S. P. Parkin, E. S. Toberer, T. McQueen, S. D. Wilson, and M. N. Ali, Anisotropic proximity-induced superconductivity and edge supercurrent in Kagome metal, $\text{K}_{1-x}\text{V}_3\text{Sb}_5$, *Sci. Adv.* **9**, eadg7269 (2023).
- [49] M. Sato, Topological odd-parity superconductors, *Phys. Rev. B* **81**, 220504 (2010).
- [50] K. Matano, M. Kriener, K. Segawa, Y. Ando, and G.-Q. Zheng, Spin-rotation symmetry breaking in the superconducting state of $\text{Cu}_x\text{Bi}_2\text{Se}_3$, *Nat. Phys.* **12**, 852 (2016).
- [51] Y. Pan, A. M. Nikitin, G. K. Araizi, Y. K. Huang, Y. Matsushita, T. Naka, and A. de Visser, Rotational symmetry breaking in the topological superconductor $\text{Sr}_x\text{Bi}_2\text{Se}_3$ probed by upper-critical field experiments, *Sci. Rep.* **6**, 28632 (2016).
- [52] S. Yonezawa, K. Tajiri, S. Nakata, Y. Nagai, Z. Wang, K. Segawa, Y. Ando, and Y. Maeno, Thermodynamic evidence for nematic superconductivity in $\text{Cu}_x\text{Bi}_2\text{Se}_3$, *Nat. Phys.* **13**, 123 (2017).
- [53] G. Du, Y. Li, J. Schneeloch, R. D. Zhong, G. Gu, H. Yang, H. Lin, and H.-H. Wen, Superconductivity with two-fold symmetry in topological superconductor $\text{Sr}_x\text{Bi}_2\text{Se}_3$, *Sci. China Phys. Mech. Astron.* **60**, 037411 (2017).
- [54] Y. Xiang, Q. Li, Y. Li, W. Xie, H. Yang, Z. Wang, Y. Yao, and H.-H. Wen, Twofold symmetry of c-axis resistivity in topological kagome superconductor CsV_3Sb_5 with in-plane rotating magnetic field, *Nat. Commun.* **12**, 6727 (2021).
- [55] S. Ni, S. Ma, Y. Zhang, J. Yuan, H. Yang, Z. Lu, N. Wang, J. Sun, Z. Zhao, D. Li, S. Liu, H. Zhang, H. Chen, K. Jin, J. Cheng, L. Yu, F. Zhou, X. Dong, J. Hu, H.-J. Gao *et al.*, Anisotropic superconducting properties of kagome metal CsV_3Sb_5 , *Chin. Phys. Lett.* **38**, 057403 (2021).
- [56] C.-w. Cho, J. Shen, J. Lyu, O. Atanov, Q. Chen, S. H. Lee, Y. S. Hor, D. J. Gawryluk, E. Pomjakushina, M. Bartkowiak, M. Hecker, J. Schmalian, and R. Lortz, Z_3 -vestigial nematic order due to superconducting fluctuations in the doped topological insulators $\text{Nb}_x\text{Bi}_2\text{Se}_3$ and $\text{Cu}_x\text{Bi}_2\text{Se}_3$, *Nat. Commun.* **11**, 3056 (2020).
- [57] M. Hecker and J. Schmalian, Vestigial nematic order and superconductivity in the doped topological insulator $\text{Cu}_x\text{Bi}_2\text{Se}_3$, *npj Quantum Mater.* **3**, 26 (2018).
- [58] T. Asaba, B. J. Lawson, C. Tinsman, L. Chen, P. Corbae, G. Li, Y. Qiu, Y. S. Hor, L. Fu, and L. Li, Rotational Symmetry Breaking in a Trigonal Superconductor Nb-Doped Bi_2Se_3 , *Phys. Rev. X* **7**, 011009 (2017).
- [59] T. Le, Y. Sun, H.-K. Jin, L. Che, L. Yin, J. Li, G. Pang, C. Xu, L. Zhao, S. Kittaka, T. Sakakibara, K. Machida, R. Sankar, H. Yuan, G. Chen, X. Xu, S. Li, Y. Zhou, and X. Lu, Evidence for nematic superconductivity of topological surface states in PbTaSe_2 , *Sci. Bull.* **65**, 1349 (2020).
- [60] Y. Song, T. Ying, X. Chen, X. Han, X. Wu, A. P. Schnyder, Y. Huang, J.-G. Guo, and X. Chen, Competition of Superconductivity and Charge Density Wave in Selective Oxidized CsV_3Sb_5 Thin Flakes, *Phys. Rev. Lett.* **127**, 237001 (2021).
- [61] Y. Luo, S. Peng, S. M. L. Teicher, L. Huai, Y. Hu, Y. Han, B. R. Ortiz, Z. Liang, Z. Wei, J. Shen, Z. Ou, B. Wang, Y. Miao, M. Guo, M. Hashimoto, D. Lu, Z. Qiao, Z. Wang, S. D. Wilson, X. H. Chen, and J. F. He, Electronic states dressed by an out-of-plane supermodulation in the quasi-two-dimensional kagome superconductor CsV_3Sb_4 , *Phys. Rev. B* **105**, L241111 (2022).
- [62] W. Kuang, G. Lopez-Polin, H. Lee, F. Guinea, G. Whitehead, I. Timokhin, A. I. Berdyugin, R. Krishna Kumar, O. Yazzev, N. Walet, A. Principi, A. K. Geim, and I. V. Grigorieva, Magnetization signature of topological surface states in a non-symmorphic superconductor, *Adv. Mater.* **33**, 2103257 (2021).
- [63] Y. Xing, Z. Shao, J. Ge, J. Luo, J. Wang, Z. Zhu, J. Liu, Y. Wang, Z. Zhao, J. Yan, D. Mandrus, B. Yan, X. Liu, M. Pan, and J. Wang, Surface superconductivity in the type II Weyl semimetal TaIrTe_4 , *Natl. Sci. Rev.* **7**, 579 (2020).